

All lit up: A nucleobase-specific recognition system has been constructed by combining DNA/RNA-binding fluorescent reporter ligands and oligonucleo-

tide conjugates bearing β -cyclodextrin (see scheme). The two molecules work cooperatively to recognize and signal the presence of specific nucleobases.

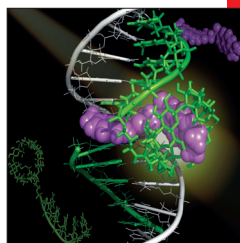
Biosensors

A. Futamura, A. Uemura, T. Imoto, Y. Kitamura, H. Matsuura, C.-X. Wang, T. Ichihashi, Y. Sato, N. Teramae, S. Nishizawa,* T. Ihara*... ■■■■-■■■■

Rational Design for Cooperative Recognition of Specific Nucleobases Using β -Cyclodextrin-Modified DNAs and Fluorescent Ligands on DNA and RNA Scaffolds



CHEMISTRY
A EUROPEAN JOURNAL
19/0 2013



WILEY-VCH

A Journal of
ChemPhysSoc
Europe
Registered by
ACES
www.chemistry-journal.com

A binary fluorimetric method.....for DNA and RNA analysis is proposed based on the combination of two probes designed to work cooperatively. One is an oligonucleotide conjugate bearing a β -cyclodextrin. The other is a small reporter ligand, which comprises linked molecules of a nucleobase-specific heterocycle and an environment-sensitive fluorophore. The reporter ligand recognizes a single nucleobase displayed in a gap on the target labeled with the conjugate, and the fluorophore moiety forms a luminous inclusion complex with nearby cyclodextrin. For more details see the Full Paper by S. Nishizawa, T. Ihara et al. on page ■■ ff.



DOI: 10.1002/chem.201300985

Rational Design for Cooperative Recognition of Specific Nucleobases Using β -Cyclodextrin-Modified DNAs and Fluorescent Ligands on DNA and RNA Scaffolds

Akika Futamura,^[a] Asuka Uemura,^[a] Takeshi Imoto,^[a] Yusuke Kitamura,^[a, b]
Hirotaka Matsuura,^[a] Chun-Xia Wang,^[c] Toshiki Ichihashi,^[c] Yusuke Sato,^[c]
Norio Teramae,^[c] Seiichi Nishizawa,^{*,[c]} and Toshihiro Ihara^{*,[a, b]}

Abstract: We propose a binary fluorimetric method for DNA and RNA analysis by the combined use of two probes rationally designed to work cooperatively. One probe is an oligonucleotide (ODN) conjugate bearing a β -cyclodextrin (β -CyD). The other probe is a small reporter ligand, which comprises linked molecules of a nucleobase-specific heterocycle and an environment-sensitive fluorophore. The heterocycle of the reporter ligand recognizes a single nucleobase displayed in a gap on the target labeled with the

conjugate and, at the same time, the fluorophore moiety forms a luminous inclusion complex with nearby β -CyD. Three reporter ligands, **MNDS** (naphthyridine–dansyl linked ligand), **MNDB** (naphthyridine–DBD), and **DPDB** (pyridine–DBD), were used for DNA and RNA probing with 3'-end or 5'-end modified β -CyD–ODN conju-

Keywords: biosensors • cyclodextrin • DNA recognition • fluorescence • host–guest systems

gates. For the DNA target, the β -CyD tethered to the 3'-end of the ODN facing into the gap interacted with the fluorophore sticking out into the major groove of the gap site (**MNDS** and **DPDB**). Meanwhile the β -CyD on the 5'-end of the ODN interacted with the fluorophore in the minor groove (**MNDB** and **DPDB**). The results obtained by this study could be a guideline for the design of binary DNA/RNA probe systems based on controlling the proximity of functional molecules.

Introduction

Various fluorescent molecular probes have been developed for targeting certain biomolecules, cell organelles, or intracellular processes.^[1–5] In general, free or nonspecifically bound probes must be thoroughly washed from the substrates on which the targets are immobilized to obtain a signal with a good contrast, because of signal interference from unbound or nonspecific probes. However, for targets dissolved or dispersed in homogeneous solutions, washing

cannot be used to separate bound and free targets. Probes for use in solution are expected to emit a signal only when they bind to their targets.^[6–12] This is an essential requirement for bioprobes providing a spatiotemporal response.

In the design of molecular probes, the structural requirements for binding to the target and for signal generation are often different. Most of the molecular probes that are widely used in current molecular biological research meet one of the two requirements. However, it is very difficult to design probes that meet both requirements in one molecule.^[13–22]

We propose a general solution for designing molecular probes that recognize their targets and switch their signal on at the same instant. This could be achieved using cooperative action between probes. We have shown the validity of the design through the analysis of DNA and RNA. To date, several DNA-probing systems based on specific photochemical reactions,^[23–25] luminous metal complex formation,^[26,27] and electrochemically modulated inclusion-complex formation^[28] on DNA have been proposed.

In this work, a convenient technique for SNP (single nucleotide polymorphism) genotyping in a homogeneous solution is presented. We prepared DNA conjugates, β -cyclodextrin (β -CyD)-modified oligodeoxyribonucleotides (**CyD-ODN**), and nucleobase-specific fluorescent reporter ligands and used them simultaneously for SNP analysis in aqueous solution. The reporters are linked hybrid molecules consist-

[a] A. Futamura, A. Uemura, T. Imoto, Dr. Y. Kitamura, Dr. H. Matsuura, Prof. Dr. T. Ihara
Department of Applied Chemistry and Biochemistry
Graduate School of Science and Technology, Kumamoto University
Kurokami, Chuo-ku, Kumamoto 860-8555 (Japan)
Fax: (+81)96-342-3679 (office) or 3873
E-mail: toshi@chem.kumamoto-u.ac.jp

[b] Dr. Y. Kitamura, Prof. Dr. T. Ihara
CREST Japan Science and Technology Agency
Gobancho, Chiyoda-ku, Tokyo 102-0076 (Japan)

[c] Dr. C.-X. Wang, T. Ichihashi, Dr. Y. Sato, Prof. Dr. N. Teramae, Prof. Dr. S. Nishizawa
Department of Chemistry, Graduate School of Science
Tohoku University, Aoba-ku, Sendai 980-8578 (Japan)
E-mail: nishi@m.tohoku.ac.jp

Supporting information for this article is available on the WWW under <http://dx.doi.org/10.1002/chem.201300985>.

ing of two parts: a nucleobase-specific heterocyclic ligand and an environment-sensitive fluorophore. In this assay, SNP bases (N: A, T, G, or C) on the targets are displayed at a gap in ternary duplexes (N-gap duplexes) consisting of the targets (DNA or RNA), the **CyD-ODN**, and the mask, as shown in Figure 1. That is, the sequences of the **CyD-ODN** and the mask are designed to be complementary to both sequences adjacent to the SNP base on the target (Figure 2a). Therefore, both ODNs (oligodeoxyribonucleic acids) form a

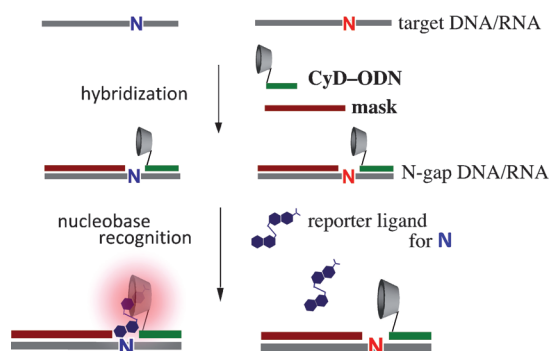


Figure 1. Schematic of nucleobase detection by binary probing. N indicates the target nucleobase: A, T, G, or C.

stable tandem duplex, regardless of the type of N. The reporter ligand is then added to these ternary duplexes with a displayed SNP base. The fluorophore moiety of the reporter is expected to form a luminous inclusion complex with nearby a β -CyD^[29–35] only when the heterocyclic moiety binds to the N displayed in the gap. Base discrimination is not based on the hybridization specificity of a long DNA probe, as in conventional methods, but on the complementarity of a small ligand with only one displayed base. This would be expected to increase the contrast of the signal.

In our previous report, we showed the preliminary result of the system, in which G-specific detection was performed by the combined use of **MNDS** (Figure 2b) and 3'-modified **CyD-ODN** (**3CyD-ODN**). The system, however, did not work with 5'-modified **CyD-ODN** (**5CyD-ODN**).^[36] We thought that the disparity between **3CyD-ODN** and **5CyD-ODN** would be derived from the asymmetric microenvironment around the gap of the DNA duplex. The orientations of the bound reporter ligand and the modified ends of β -CyD might explain the results. Here, we conducted a systematic study using three reporter ligands, **MNDS** and two newly prepared ligands **MNDB** and **DPDB**, having different binding selectivities and fluorophores. The method provides a general principle for the rational design of systems for nucleobase targeting of DNA or RNA. In this report, the results for all of the three ligands are shown in a comprehensive style to ensure the completeness of the whole picture of the bimolecular probing scheme.

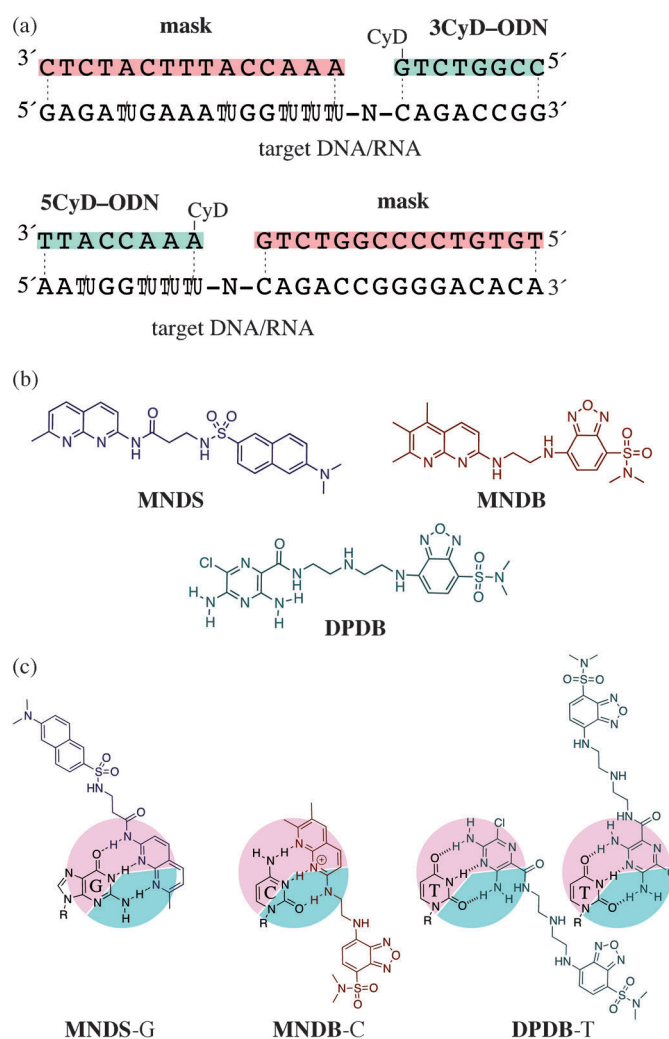


Figure 2. Probes and targets. a) Sequences of the ODN probes (green line, **CyD-DNA**; red line, **mask**) and the target DNA and RNA. N indicates the target nucleobase: A, T, G, or C. b) Structures of fluorescent reporter ligands: **MNDS**, **MNDB**, and **DPDB**. c) Putative pairings of the fluorescent reporters and nucleobases. The red and green areas indicate major and minor grooves, respectively.

Results and Discussion

Design of the system: Figure 2a, b show the sequences and structures of the ODNs and the three fluorescent reporter ligands used in this study. Figure 2c shows putative pairings of the fluorescent reporters and nucleobases. Part of the sequence of the *TPMT* gene was used as a target. SNP bases, N, on the targets are displayed in a gap in the duplexes (N-gap) consisting of the targets **CyD-ODN** and **mask**. That is, the sequences of **CyD-ODN** and **mask** are designed to be complementary to both sequences adjacent to the N on the target. Both ODNs form a fully matched tandem duplex regardless of the type of N. The **mask** is expected to play a role to define the target base to the one adjacent to **CyD-ODN** and to form a comfortable space to accommodate the reporter ligands.

Fluorescent reporter molecules were systematically designed by covalently linking two functionally different elements, a heterocycle enabling complementary hydrogen bonding with a particular nucleobase and an environment-sensitive fluorophore. As heterocycles for nucleobase recognition, 1,8-naphthyridine (MND) and 3,5-diamino-6-chloropyridine (DAP) were used. MND binds with G or C depending on the structure of the linker chain tethered to the fluorophore moiety.^[37] DAP is complementary to T/U.^[17] The binding behavior of these heterocycles has been studied in detail separately for the nucleobases in an AP site (apurinic/aprimidinic site). The selectivity and the binding affinities were investigated in regard to the effect of the introduction of functional groups^[16,38–40] and flanking nucleobases.^[39–43] At the same time, 2,6-dansyl and 4-(*N,N*-dimethylaminosulfonyl)benzofurazan (DBD) were employed as environment-sensitive fluorophores. **MNDS** is a hybrid molecule of MND (monomethyl) and 2,6-dansyl, which are the base-recognition and fluorescent parts, respectively. The dansyl moiety protrudes into the major groove of the duplex, when MND forms a supposed complex with G. **MNDB** consists of MND (trimethyl) and DBD. It is expected to bind with C with its DBD moiety protruding into the minor groove. **DPDB** consists of DAP and DBD. The DBD moiety could stick out into both grooves, because the hydrogen bonding surface of T/U is symmetric. The fluorescent reporter ligands could be designed to meet the demands of different target nucleobases, fluorescent colors, and directions that the fluorophore protrudes by simply combining the elementary functional modules.

Interaction of MNDS with N-gap DNA duplexes: Figure 3a (top) shows the fluorescence spectra of **MNDS** in the presence of N-gap duplexes with the **3CyD-ODN** (left) and **5CyDODN** (right), measured at 0°C. Normalized fluorescence intensities at 443 nm are shown as the relative values in the bar graph (bottom) after subtraction of the fluorescence intensity of the solution containing only **MNDS**. The signal was enhanced significantly only for G-target DNA when using the **3CyD-ODN**. As expected, the MND moiety in **MNDS** seemed to recognize G by complementary hydrogen bonding in the gap. The relative fluorescence signals (with respect to G) for A, C, and T were 10.7, 11.6, and 22.7, respectively. The signal from dansyl moiety was observed as blue emission, and the contrast is large enough to be recognized by the naked eye, as shown in Figure 3b. On the other hand, the specific signal was not observed when using the **5CyD-ODN**.

The interactions of **MNDS** with the G-gap DNA duplexes were further studied by fluorescence titration at 0°C (see Figure S1 in the Supporting Information). The observed spectral changes resulted from the formation of an inclusion complex between the dansyl and β -CyD moieties, because the **MNDS** spectra scarcely changed by the addition of the control G-gap duplex lacking β -CyD. The changes in the fluorescence intensities were fitted to the theoretical curve, which was derived assuming a 1:1 interaction. The binding

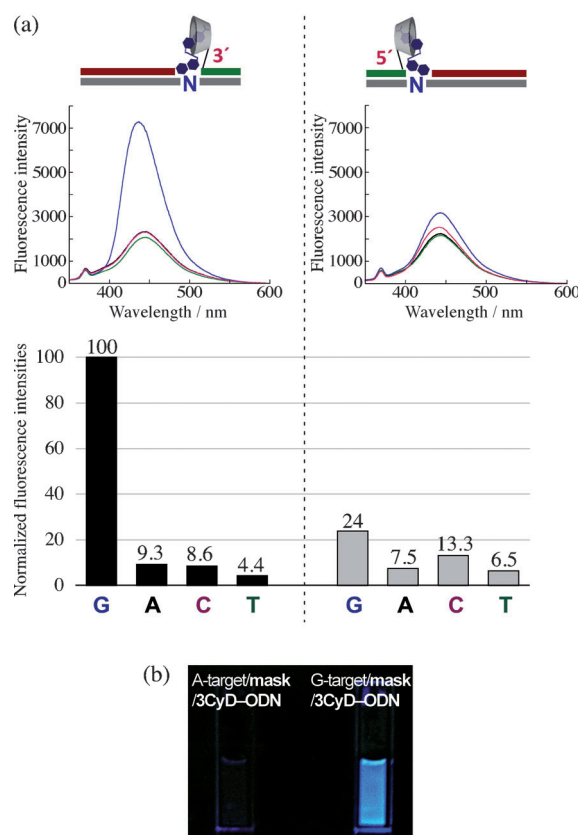


Figure 3. Fluorometric DNA analysis using **MNDS**. a) Fluorescence spectra (top) (blue, G-target; black, A-target; red, C-target; green, T-target DNA) and normalized fluorescence intensities at 443 nm. Left and right indicate the results for the detection of N-target DNAs using **3CyD-ODN** and **5CyD-ODN** conjugates, respectively. 1.0 μ M N-gap duplexes, 5.0 μ M **MNDS**, 1 M NaCl, 10 mM phosphate buffer (pH 7.0), 0.83% DMSO, $\lambda_{\text{ex}} = 328$ nm, 0°C. b) Fluorescence images of the solutions of A-target (left) and G-target DNAs (right) with **3CyD-ODN** measured at 5°C. Excitation source: low-pressure mercury lamp (6 W, 365 nm).

constants of **MNDS** with β -CyD and **MNDS** with a G-gap duplex containing **3CyD-ODN** were calculated to be $5.2 \times 10^2 \text{ M}^{-1}$ and $2.4 \times 10^5 \text{ M}^{-1}$, respectively. These results show the validity of the molecular design of **MNDS**. Although the binding of each elemental unit of **MNDS**, MND and dansyl, with its supposed counterpart, G-gap and β -CyD, is very weak, the synergistic effect of linking the two elements made the binding constant of their integrated hybrid molecule, **MNDS**, significantly higher in the microenvironment of G-gap duplex with the **3CyD-ODN**. That is, MND inserts into the G-gap to form complementary hydrogen bonding with G and, simultaneously, the dansyl group is accommodated in the nearby β -CyD modified at the 3'-end of the ODN. The binding constants with A-, C-, and T-gap duplexes carrying the **3CyD-ODN** were too small to be calculated. Meanwhile, the binding constant of **MNDS** with the G-gap duplex containing the **5CyD-ODN** was much less than that with the **3CyD-ODN**. It was roughly estimated to be $< 10^4 \text{ M}^{-1}$. Therefore, the difference in fluorescence signal intensities observed for **3CyD-ODNs** and **5CyD-ODNs**

shown in Figure 3a could be attributed to the difference in the binding constant for both duplexes. Thus, each of the two elementary units of **MNDS** does not contribute sufficiently to the **MNDS** binding in the G-gap duplex with the **5CyD-ODN**. The poor signal contrast observed for the **5CyD-ODN** system could be the result of inadequate interaction of the MND moiety with N-gaps and/or dansyl with β -CyD.

To explain the disparity observed in the interaction of **MNDS** with **3CyD-ODN** and **5CyD-ODN**, the steric effect derived from the asymmetric nature of the DNA duplex structure may have to be taken into account. **MNDS** protrudes its dansyl moiety into the major groove of the duplex when MND forms complementary hydrogen bonds with G in the gap, as shown in Figure 4. The distances from the ends of both ODNs that face into the gap to the dansyl

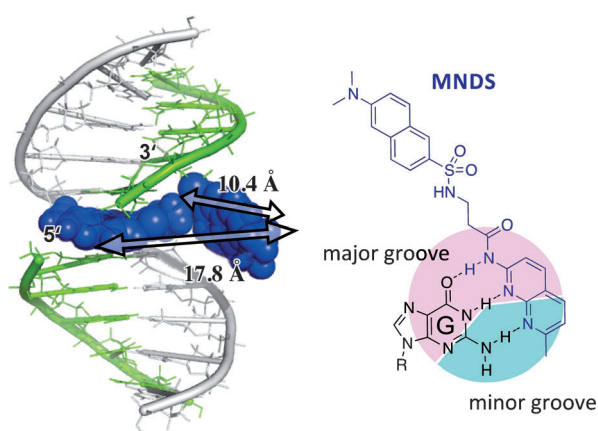


Figure 4. One of the possible 3D structures of the **MNDS**/G-gap DNA duplex. The model was geometry-optimized by AMBER* force field with a GB/SA (generalized Born/surface area) solvent model using MacroModel version 9.1. The distances from the dansyl moiety of bound **MNDS** to both (3'- and 5'-) ends of ODNs are quite different. β -CyD moiety of the **CyD-ODN** was omitted from the structure for clarity.

group of the bound **MNDS** would be quite different. Molecular modeling studies showed that the distances from the 3'- and 5'-ends of both ODNs to the center of dansyl were about 10.4 and 17.8 Å, respectively, in the optimized complex structure, in which the short linker chain of **MNDS** took a trans conformation. The conformational freedom would be limited for the linker chain that connects the 5'-end of the ODN with β -CyD, when the dansyl group of **MNDS** is included in the 5'-modified β -CyD. This would make the binding of **MNDS** with the G-gap duplex of the **5CyD-ODN** weaker, because this entropic disadvantage would deteriorate the synergy between the two elementary units of **MNDS** on binding to the G-gap duplexes. The results suggest that while the reporter ligand that protrudes its fluorophore into the major groove of the N-gap duplex works cooperatively with the **3CyD-ODN**, the ligand that protrudes its fluorophore into the minor groove works with the **5CyD-ODN**. The former case has been verified with

MNDS. The latter case needs to be demonstrated by experiments using other reporter ligands.

Interaction of MNDB with N-gap DNA duplexes: To complete the working principle of the system derived from the unique binding behavior of **MNDS**, we prepared new fluorescent reporter molecules, **MNDB** and **DPDB** (see Figure 2 and the next section). **MNDB** consists of MND and DBD as recognition and signaling moieties, respectively. The resonance effect from the amino linker of **MNDB** raises the basicity of the endocyclic nitrogens of MND and changes the target nucleobase to C. **MNDB** protrudes the DBD moiety into the minor groove when it forms a complementary pairing with C displayed in the gap, as shown in Figure 2c. According to the hypothetical principle mentioned above, the DBD moiety in **MNDB** would be accommodated into the β -CyD of a **5CyD-ODN**.

Figure 5a shows the fluorescence spectra and normalized fluorescence intensities of **MNDB** in the presence of N-gap DNA duplexes with the **3CyD-ODN** (left) and the **5CyD-**

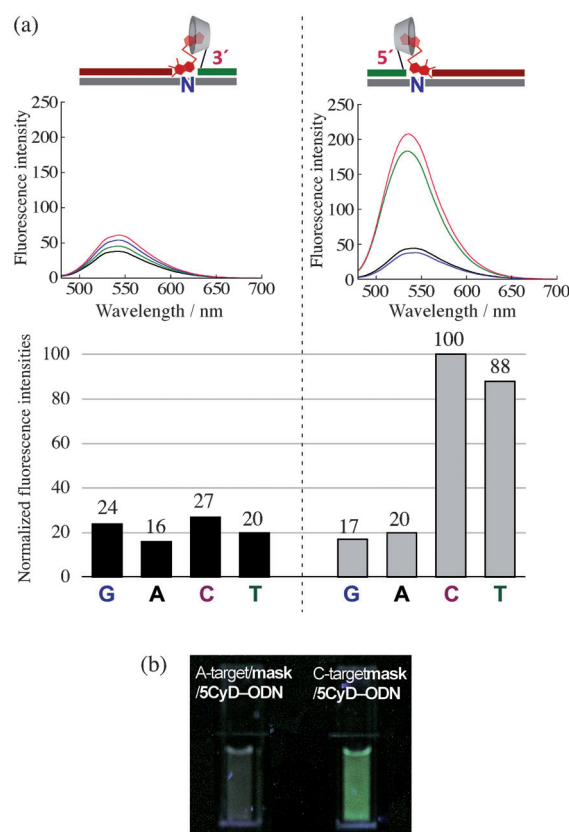


Figure 5. Fluorometric DNA analysis using **MNDB**. a) Fluorescence spectra (blue, G-target; black, A-target; red, C-target; green, T-target DNA) and normalized fluorescence intensities of **MNDB** at 535 nm. Left and right indicate the results for the N-target DNAs detection using **3CyD-ODN** and **5CyD-ODN** conjugates, respectively. 1.0 μ M N-gap duplexes, 5.0 μ M **MNDB**, 1 M NaCl, 10 mM phosphate buffer (pH 7.0), 0.83% DMSO, $\lambda_{\text{ex}} = 447$ nm, 0°C. b) Fluorescence images of the solutions of tandem duplexes of A-target (left) and C-target DNA (right) containing the **5CyD-ODN** in the presence of **MNDB** at 5°C. Excitation source: low-pressure mercury lamp (6 W, 365 nm).

ODN (right). The signal was enhanced significantly not only upon addition of the C-target but also the T-target in the presence of the **5CyD-ODN**. Signal changes observed in the interaction with A- and G-targets were very small. A dual response to C and T could be caused by protonation on two different endocyclic nitrogens of MND. While protonation of the N1 position makes MND complementary to C, protonation of the N8 position makes it complementary to T. Actually, an MND derivative is known to bind to both C and T in the AP site of a DNA duplex with binding constants of 1.9×10^7 and $0.91 \times 10^7 \text{ M}^{-1}$, respectively.^[16] The emission from the DBD moiety was observed as a green image, as shown in Figure 5b. By contrast, selective recognition of the nucleobases failed in the presence of the **3CyD-ODN**. The interactions of **MNDB** with the C-gap duplexes were studied further by fluorescence titration at 0 °C (see Figure S2 in the Supporting Information). The binding constants of **MNDB** with the C-gap and T-gap duplexes carrying the **5CyD-ODN** were calculated to be 1.8×10^5 and $1.3 \times 10^5 \text{ M}^{-1}$, respectively. Meanwhile, the binding constant of **MNDB** with the A-gap duplex was too small to be calculated. Incidentally, the binding constant of **MNDB** with β -CyD was estimated to be $4.3 \times 10^3 \text{ M}^{-1}$ under the same conditions (data not shown). These results indicate that pyrimidines (C and T) could be detected by the combined use of **MNDB** and the **5CyD-ODN**.

Thus, we have completed the entire picture of recognition/signaling for the target nucleobases using the combination of a fluorescent reporter ligand and a **CyD-ODN**. That is, **3CyD-ODNs** and **5CyD-ODNs** form luminous inclusion complexes with the reporter ligands at the major and minor grooves, respectively, of N-gap DNA duplexes. According to this simple principle, the system can be logically designed to detect specific nucleobases.

Interaction of DPDB with N-gap DNA duplexes: **DPDB** was designed to target T, based on the principle mentioned above. **DPDB** consists of DAP and DBD as recognition and signaling moieties, respectively. As shown in Figure 2c, bimodal binding is expected for **DPDB** on T recognition, because the hydrogen bonding surface of T is symmetric (as is that of DAP). Therefore, **DPDB** might work cooperatively with both **3CyD-ODNs** and **5CyD-ODNs**, because **DPDB** is allowed to direct the DBD moiety to either groove.

Figure 6 shows the fluorescence spectra of **DPDB** and the normalized fluorescence intensities at 550 nm with the addition of N-target DNAs in the presence of the **3CyD-ODN** (left) and the **5CyD-ODN** (right). As expected, the signal was enhanced significantly only for the T-target with both the **3CyD-ODN** and **5CyD-ODN**. Signal changes observed for the interactions with A-, C-, and G-targets were marginal. The binding constants of **DPDB** with the T-gap DNA duplexes carrying the **3CyD-ODN** and the **5CyD-ODN** were calculated as 2.1×10^7 and $9.2 \times 10^5 \text{ M}^{-1}$, respectively (see Figure S3 in the Supporting Information). The interaction of **DPDB** and other N-gap DNA duplexes carrying the **3CyD-ODN** or the **5CyD-ODN** were examined in the same way.

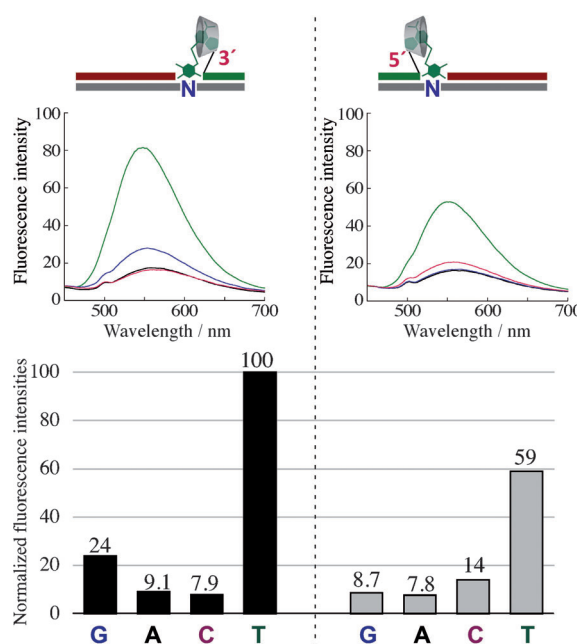


Figure 6. Fluorescence spectra (blue, G-target; black, A-target; red, C-target; green, T-target DNA) and normalized fluorescence intensities of **DPDB** at 550 nm. Left and right show the results for the N-target DNA detection using **3CyD-ODN** and **5CyD-ODN** conjugates, respectively. $1.0 \mu\text{M}$ N-gap duplexes, $5.0 \mu\text{M}$ **DPDB**, 1 M NaCl, 10 mM phosphate buffer (pH 7.0), 0.83% DMSO, $\lambda_{\text{ex}} = 427 \text{ nm}$, 0°C .

Their binding constants were too small to be calculated. Separately, the binding constant of **DPDB** with β -CyD was estimated to be $8.8 \times 10^2 \text{ M}^{-1}$ under the same conditions. **DPDB** binding to both T-gap DNA duplexes seems to be enhanced by a synergistic effect of both constituents, DAP and DBD.

The working principles of the fluorescent reporter ligands in the binary probing system, which were derived from the studies of **MNDS** and **MNDB**, were supported by the **DPDB** studies. We confirmed that the effective interactions involving the 3'- and 5'-ends of ODNs facing the N-gap occur at the major and the minor grooves, respectively (Figure 7).

Binary probing for RNA targets: This system can also be used to detect RNA targets with the same sequences. Hence, DNA/RNA heteroduplexes were used as scaffolds for nucleobase recognition. Figure 8 shows the normalized fluorescence intensities of the three reporter ligands for N-target RNAs using the **3CyD-ODN** (left) and the **5CyD-ODN** (right). Measurements were performed under the same conditions used for the DNA targets mentioned above. Results obtained for RNA targets were totally different from those for the DNA targets. The most pronounced difference from the DNA targets was shown in the response of **MNDS** (Figure 8a). **MNDS** did not work with either of the **CyD-ODNs** in the heteroduplex systems. None of the RNA targets increased the fluorescence signal of **MNDS**. Meanwhile, although the pyrimidine-specific response of

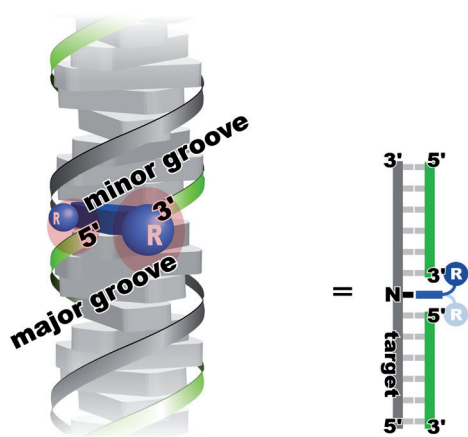


Figure 7. Simplified 3D image of the gap in the tandem DNA duplex. The target nucleobase, N, is displayed in the gap. The nucleobase-specific fluorescent ligands (blue) inserted into the gap protrude their fluorophores (shown as "R") into the major or minor groove. The fluorophores in the major and the minor groove locate in close proximity with the 3'- and 5'-end of the probe ODNs (green), respectively.

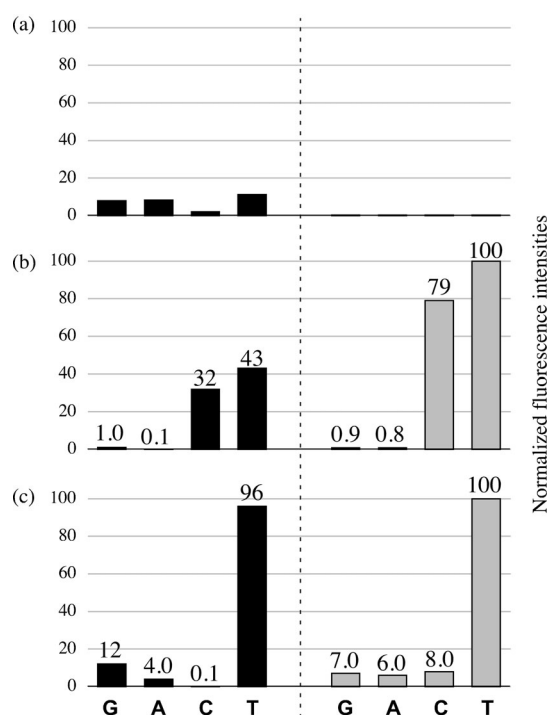


Figure 8. Normalized fluorescence intensities of a) MNDS, b) MNDB, and c) DPDB for N-target RNAs detection. Left and right indicate the results obtained using the 3CyD-ODN and the 5CyD-ODN, respectively. Fluorescence of each reporter molecule (5.0 μM) with N-gap heteroduplexes (1.0 μM) was measured in a solution containing NaCl (1 M), phosphate buffer (10 mM, pH 7.0), and DMSO (0.83%) at 0 °C. λ_{exc} = 328, 447, and 427 nm for MNDS, MNDB, and DPDB, respectively.

MNDB was preserved for the RNA targets, the fluorescence was enhanced not only with the 5CyD-ODN but also with the 3CyD-ODN (Figure 8b). Response characteristics of DPDB for RNA targeting were almost the same as those

Table 1. Nucleobases that can be targeted by the binary probing system for DNA and RNA.^[a]

Target	Conjugate	Reporter ligand		
		MNDS	MNDB	DPDB
DNA	5CyD-ODN	–	C, T (m)	T (m)
	3CyD-ODN	G (M)	–	T (M)
RNA	5CyD-ODN	–	C, T (m)	U (m)
	3CyD-ODN	–	C, T (m)	U (m)

[a] M and m in parentheses show the putative grooves, where the two probes (the conjugate and the reporter ligand) meet with each other. They stand for major (M) and minor (m) grooves.

with DNA (Figure 8c). DPDB showed a specific response to U using either the 3CyD-ODN or the 5CyD-ODN.

The profiles for DNA and RNA recognition are summarized in Table 1. The profiles of DNA and RNA with the same sequence were very different from each other. UV melting studies showed that all the duplexes (N-gap homoduplexes) are stable under the experimental conditions (data not shown). Therefore, the difference in the response might come from the differences in the structures of the DNA duplexes and DNA/RNA heteroduplexes. Figure 9 shows CD spectra of the G-gap duplexes lacking β -CyD. In the case of the DNA homoduplexes, the spectrum showed a positive peak around 280 nm and an intense negative peak around 250 nm (Figure 9a). The CD spectrum of the RNA/DNA heteroduplex indicated an intense positive peak

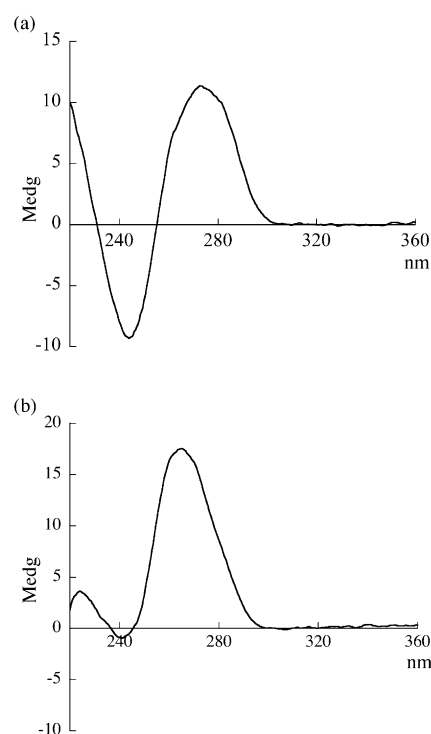


Figure 9. CD spectra of G-gap duplexes lacking β -CyD: a) DNA homoduplex and b) RNA/DNA heteroduplex. The duplexes were dissolved (1.25 μM) in a solution containing NaCl (1.0 M), phosphate buffer (10 mM, pH 7.0), and DMSO (0.83%). Measurements were carried out at ambient temperature.

around 275 nm and a small negative peak around 230 nm (Figure 9b). These are the typical features of B-form and A-form duplexes.^[44,45] That is, N-gap DNA homoduplexes and RNA/DNA heteroduplexes used in this study should take the structures of B-form and A-form duplexes, respectively. One of the notable features of an A-form duplex is that the major groove is extremely narrow and very deep, while the minor groove is very broad and shallow.^[46,47] This structure might explain the signal profile for RNA. **MNDS** protrudes its dansyl moiety to the major groove. A modeling study showed that the narrow and deep major groove of the heteroduplex does not leave space for β -CyD after the dansyl moiety sticks out (Figure 10a). Therefore, β -CyD could not

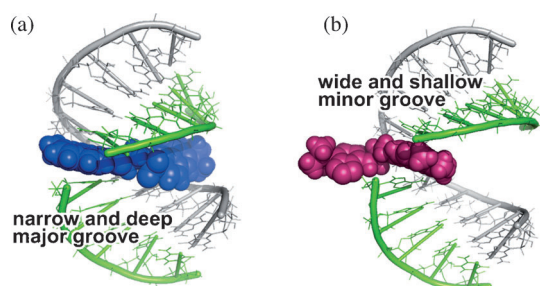


Figure 10. One of the possible 3D structures of a) **MNDS**/G-gap and b) **MNDB**/C-gap RNA/DNA heteroduplexes. The model was geometry-optimized by AMBER* force field with GB/SA (generalized Born/surface area) solvent model using MacroModel version 9.1. The fluorophore of **MNDS** is buried deeply in the major groove of the heteroduplex, while that of **MNDB** is exposed to the bulk solution from the shallow minor groove of the heteroduplex. The β -CyD moiety of the **CyD-ODN** was omitted from the structure for clarity.

access the dansyl moiety in the major groove of the heteroduplex, even from the 3'-end of **CyD-ODN**. The DBD moiety of **MNDB** protrudes into the minor groove. The DBD in the shallow minor groove seems to be accessible from both 3'- and 5'-ends of the **CyD-ODNs**, as shown in Figure 10b. Only the reporter ligands that protrude their signaling group into the minor groove could be used for RNA analysis.

Effect of temperature on the signal contrast: One of the merits of the present method is that the measurements for all of the targets using different DNA probes could be performed under the same conditions, because the recognition does not rely on subtle differences in thermal stabilities of the duplexes formed with the probes. Generally, DNA probing relies on the specificity of probe hybridization. Accordingly, to recognize one-base displacement, the temperature should be controlled in a narrow range between the melting temperatures of the full match and mismatch duplexes. In the present system, however, all the duplexes that interact with the reporter ligands are fully matched duplexes; only the unpaired base displayed in the gap is different. Therefore, the response is not completely independent of temperature, but the temperature range in which we can conduct

the SNP assay should be quite wide compared with traditional probe hybridization. Fluorometric SNP analyses using **MNDS** and **3CyD-ODN**, for example, were performed to investigate an effect of the temperature on the signal contrast of this system. Normalized signals measured at different temperatures are shown in Figure 11 with the UV melting curve of the duplex. The signal quality (signal contrast) did not deteriorate much, even at 35°C, which is below the

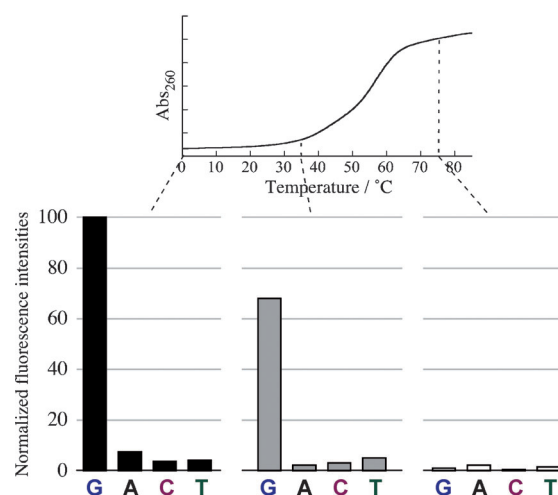


Figure 11. UV melting curve (top) and normalized fluorescence intensities (bottom) of **MNDS** in the presence of N-gap duplexes containing the **3CyD-ODN**. Fluorescence measurements were performed at 0°C (left), 35°C (center), and 75°C (right). All other experimental conditions were the same as Figure 3.

melting temperature ($T_m \approx 50^\circ\text{C}$) of this duplex. The measurement at 75°C was, of course, disabled. Thus, the assay can be carried out at any temperature that is lower than the T_m , because the duplex framework that provides the environment for nucleobase recognition/signaling is formed at temperatures below the T_m . The temperature dependence of the interaction of **MNDS** with G-gap DNA duplex also has to be taken into account. The decrease in the signal intensities at 35°C compared with those at 0°C observed in Figure 11 can be attributed to the temperature dependence of **MNDS** binding. As commonly observed in most bimolecular interactions, the bindings of MND and dansyl with the G-gap and β -CyD, respectively, are thought to weaken with a rise in temperature. However, the result showed that the temperature dependence of the **MNDS** binding was not so significant, at least in the temperature range of the present measurements. Even so, the measurement at 0°C is the most desirable condition, which endorses a highest stabilization for all the duplexes in aqueous solutions. This unique feature (low temperature susceptibility) could be very important in massively parallel processing systems such as DNA arrays or chips.

Remaining problems and perspective: The general concerns for molecular probes are mainly selectivity and sensitivity.

To improve probes according to these two requirements, we have been conducting preliminary studies, separately, using various nucleobase-recognition ligands. For selectivity, we now have ligands that are complementary to each of the four nucleobases. For example, the C/T selectivity of naphthyridine can be controlled by introducing electron-withdrawing groups (such as a trifluoromethyl group) to the ring.^[39] The protonation to the endocyclic nitrogens of naphthyridine is delocalized between the N1 and N8 positions. The electron-withdrawing effect seems to localize the protonation to the N1 position and makes the naphthyridine ring complementary to C. We have just reported that the C/T selectivity could also be controlled by competitive binding of additional ligands.^[48] We have also published reports that alloxadine and lumazine have adenine selectivity.^[38,49] All of these findings could be fed into the present system.

The sensitivity of the present system is adequate for the products of polymerase chain reactions (PCR), but still should be improved more for practical applications. Considering the properties of the fluorophores employed in this study, the signal intensities were supposed to be enhanced more than observed here. It was apparent that only a portion of the reporter ligands bound with the N-gaps under the experimental conditions. This is due to the low binding constant of the reporter ligands to the target N-gaps. If we use ligands with higher binding constants in this system, we could reduce the concentration of the ligand and, consequently, improve the signal contrast. We already succeeded in the synthesis of such ligands for some cases.^[40] Alternatively or additionally, modification of β -CyD would be effective. For example, by making β -CyD hydrophobic (e.g., by methylation), both the binding constant and the fluorescence intensity of the inclusion complexes could be enhanced.^[50]

Conclusions

A nucleobase-specific recognition system was constructed by the rational design of a combination between DNA/RNA-binding fluorescent reporter ligands and CyD-ODN conjugates. The two molecules work cooperatively to recognize/report specific nucleobases displayed in the gap of the duplexes. The groove in which the expected cooperation proceeds can be pre-assigned according simple rules. For DNA targeting, the signaling moiety located in the major groove interacts with the counterpart modified on the 3'-end of ODN, while the reporter moiety in the minor groove interacts with that on the 5'-end of ODN. The system permits the design of various reporting molecules in a logical manner. The reporting ligands could be prepared by covalently linking the selected recognition and fluorescent molecules through an alkyl chain, because the two elementary processes (recognition and reporting) are separated and allotted to two different sites on the duplex structure. Therefore, the two elementary functional groups can be chosen in-

dependently to design the desired reporting ligands for specific nucleobases and fluorescence colors.

The design of the proposed system is general; therefore, the signal is not be limited to fluorescence. Various signals (e.g., electrochemical, colorimetric, or catalytic) could be modulated by each of the specific counterparts through the controlled proximity in the major and minor grooves of the N-gap DNA duplexes.

Experimental Section

General: β -CyD and N-succinimidyl 3-(2-pyridyldithio) propionate (SPDP) were purchased from Sigma-Aldrich (Saint Louis, MO, USA) and Dojindo Laboratories (Kumamoto, Japan), respectively. RNA targets were purchased from Japan Bio Services (Saitama, Japan). All ODNs were synthesized by an automated DNA synthesizer (Expedite 8900) using conventional phosphoramidite methods. The phosphoramidite monomers were purchased from Proligo (Hamburg, Germany) and Glen Research (Sterling, VA, USA). After purification by HPLC, all ODNs and synthesized ODN conjugates were identified using MALDI-TOF mass spectrometry on a Bruker Daltonics Autoflex-III (Billerica, MA, USA). All other reagents were obtained as the highest grade and used without further purifications.

CyD-ODNs (5CyD-ODNs and 3CyD-ODNs) were synthesized according to Scheme S1 (Supporting Information). 3'- or 5'-end aminopropyl-linked DNA was modified with a bifunctional linker molecule and then coupled with monothiolated β -CyD.

Synthesis of monotosylated β -CyD:^[50] β -CyD (0.50 g, 0.43 mmol) was dissolved in dried pyridine (4.3 mL) under an atmosphere of argon. To the solution, *p*-toluene sulfonylchloride (0.16 g, 0.85 mmol) was added in an ice bath and then stirred at room temperature. The progress of the reaction was occasionally monitored by TLC (1-butanol/ethanol/water = 5:4:3, indicator: *p*-anisaldehyde). The reaction was quenched by addition of water (0.35 mL) after 3 h. Analysis by TLC indicated the presence of the three spots corresponding to β -CyD (R_f = 0.30), monotosylated β -CyD (0.48), and ditosylated β -CyD (0.57) at almost the same density. The solution was concentrated to a half in vacuo and poured into acetone (8.5 mL) with vigorous stirring. The resulting white solid was collected and repeatedly recrystallized from water.

White solid 72 mg (12.7%); ¹H NMR (399.65 MHz, [D₆]DMSO): δ = 2.43 (s, 3H), 3.10–3.45 (m, 14H), 3.45–3.66 (m, 28H), 4.10–4.60 (m, 6H), 4.76 (s, br, 2H), 4.83 (s, br, 5H), 5.60–5.85 (m, 14H), 7.42 (d, 2H, J = 8.3 Hz), 7.74 ppm (d, 2H, J = 8.3 Hz).

Synthesis of monothiolated β -CyD:^[51,52] Monotosylated β -CyD (0.50 g, 0.39 mmol) and thiourea (0.50 g, 6.6 mmol) were dissolved in aqueous methanol (25 mL, 80%) and refluxed for 72 h. The solution was evaporated in vacuo. The solid was suspended in methanol (7.6 mL) and stirred for 1 h at room temperature. The solid was filtered and dissolved in aqueous solution of NaOH (17 mL, 10%) and stirred for 5 h at 50°C. After the solution was acidified with HCl (1M) to pH 2, trichloroethylene (1.2 mL) was added. After stirring overnight, the precipitate was filtered and washed with water. Evaporation of trichloroethylene in vacuo followed by repeated recrystallization from water gave a white solid.

White solid 0.27 g (59.4%); TLC (silica), one spot, R_f = 0.23 (CH₂CO₂Et/*n*-PrOH/H₂O, 7:7:5); MS (MALDI-TOF): m/z calcd for [M+H]⁺: 1150.54; found: 1150.06.

Synthesis of SPDP-DNA conjugate: The purified 3'- or 5'-end aminopropyl-linked ODN (100 nmol) was dissolved in carbonate Na buffer (100 μ L, 0.5M, pH 9.3). To this solution, SPDP (1.5 mg, 4.6 μ mol) dissolved in DMSO (50 μ L) was added. The resulting suspension was stirred at ambient temperature overnight. The solution was diluted to 400 μ L with water. The mixture was purified by RP-HPLC under the following conditions. Column: Wakosil-II 5C18 RS, room temperature, flow rate: 1.0 mL min⁻¹, eluent A: TEAA (triethylamine-acetic acid, 0.1M, pH 7.0),

eluent B: acetonitrile, linear gradient: 5–30% B in 30 min, detection wavelength: 260 nm.

MS (MALDI-TOF): m/z calcd for $[M-H]^-$ (3'-modified): 2746.46; found: 2746.81; m/z calcd for $[M-H]^-$ (5'-modified): 2724.50; found: 2724.37.

Synthesis of β -CyD-DNA conjugate (CyD-ODN): SPDP-DNA conjugate (50 nmol) was dissolved in phosphate-Na buffer (100 μ L, 10 mM, pH 7.2). To this solution was added monothiolated β -CyD (5.8 mg, 5.0 μ mol) dissolved in DMSO (60 μ L). The resulting suspension was stirred at ambient temperature overnight. The solution was diluted to 400 μ L with water. The mixture was purified by RP-HPLC under the following conditions. Column: Wakosil-II 5C18 RS, room temperature, flow rate: 1.0 mL min⁻¹, eluent A: 0.1 M TEAA (pH 7.0), eluent B: acetonitrile, linear gradient: 5–30% B in 30 min, detection wavelength: 260 nm.

MS (MALDI-TOF): m/z calcd for $[M-H]^-$ (3'-modified): 3771.77; found: 3770.94; m/z calcd for $[M-H]^-$ (5'-modified): 3749.81; found: 3748.90.

Synthesis of MNDS: MNDS was synthesized as described previously.^[56] The outline of the procedure is as follows. Aminonaphthyridine was coupled with activated ester of N-protected aminopropionate to form a naphthyridine connected with a protected aminolinker chain through an amide bond. After deprotection, it was coupled with dansyl chloride to obtain MNDS.

Synthesis of MNDB: MNDB was synthesized as described previously.^[53] The outline of the procedure is as follows. Aminonaphthyridine was chlorinated and then coupled with 1,2-diaminoethane to form a naphthyridine derivative with an aminolinker chain, which is tethered through the secondary amine. Finally, it was coupled with DBD-F (7-fluoro-4-(N,N-dimethylaminosulfonyl)benzofurazan) to obtain MNDB.

Synthesis of 3,5-diamino-N-(2-((2-aminoethyl)amino)ethyl)-6-chloropyrazine-2-carboxamide:^[54] Methyl-3,5-diamino-6-chloropyrazine-2-carboxylate (1.0 g, 4.9 mmol) was added to diethylenetriamine (1.5 g, 15 mmol) and stirred for 24 h at 100 °C. The solution was suspended in CHCl₃ and subsequently extracted with HCl (0.1 M). The aqueous layer was neutralized with NaOH and extracted with CHCl₃. The organic layer was concentrated in vacuo and the crude residue was purified by column chromatography on amino-group-modified silica gel (CHCl₃/MeOH). The obtained residue was identified by MALDI-TOF MS and was used for the next step without further purification.

Synthesis of DPDB: To a mixture of 3,5-diamino-N-(2-((2-aminoethyl)amino)ethyl)-6-chloropyrazine-2-carboxamide (50 mg, 0.21 mmol) and DBD-F (70 mg, 0.31 mmol) in DMF (8 mL), triethylamine (4 mL) was added and the reaction mixture was stirred and refluxed under N₂ atmosphere for 12 h. The solvent was concentrated in vacuo and the crude product was purified by column chromatography on an amino-group-modified silica gel (CHCl₃/MeOH).

Yellow solid 29 mg (28%); ¹H NMR (400 MHz, DMSO): δ = 7.87 (d, 1H, J = 7.5 Hz), 7.51 (br, 1H), 6.85 (br, 1H), 6.09 (d, 1H, J = 7.5 Hz), 5.11 (s, 2H), 3.51 (m, 2H), 3.42 (m, 2H), 3.08 (m, 2H), 2.87 (m, 2H), 2.85 ppm (s, 6H); MS (ESI): m/z calcd for C₁₇H₂₄ClN₁₀O₄S: 499.1391 $[M+H]^+$; found: 499.1386.

Circular dichroism (CD) measurements: CD spectra were obtained using a JASCO J-725 spectropolarimeter equipped with a Peltier thermal controller. CD spectra were measured from 360 to 200 nm in a 0.1 cm path length cell at 0 °C during N₂ purging to prevent moisture condensation on the cell. The concentration of the samples was 1.25 μ M in 10 mM phosphate buffer (pH 7.0) containing NaCl (1 M).

Fluorescence measurements: Fluorescence measurements were performed at 0 °C using a JASCO FP-6500 spectrofluorometer and a PerkinElmer LS55 equipped with a Peltier thermal controller during N₂ purging to prevent moisture condensation on the quartz cell. Each of the reporter molecules (5.0 μ M) was added into the solution of N-gap duplexes (1.0 μ M) dissolved in phosphate buffer (10 mM, pH 7.0), NaCl (1 M), and DMSO (0.83%), and subjected to a measurement. Normalized fluorescence intensities were estimated after subtraction of the signal of the reporter molecule alone from each measurement.

Acknowledgements

We thank Ms. M. Miyabe for assistance in the mass spectrometry measurements for CyD-ODN conjugate identification. We also thank Prof. H. Ihara and Dr. H. Jintoku for their support in measuring CD and fluorescence spectra. This work was supported by the Grant-in-Aid for Scientific Research on Innovative Areas (Coordination Programming, Area 2107) [No. 24108734 to T.I.], Scientific Research (B) [No. 24350040 to T.I.] from the Ministry of Education, Culture, Sports, Science and Technology, Japan; and the Health Labour Sciences Research Grant (Research on Publicly Essential Drugs and Medical Devices) [to T.I.] from the Ministry of Health and Labour, Japan.

- [1] D. M. Kolpashchikov, *Chem. Rev.* **2010**, *110*, 4709–4723.
- [2] A. B. Iliuk, L. Hu, W. A. Tao, *Anal. Chem.* **2011**, *83*, 4440–4452.
- [3] J. Liu, Z. Cao, Y. Lu, *Chem. Rev.* **2009**, *109*, 1948–1998.
- [4] A. C. Syvänen, *Nat. Rev. Genet.* **2001**, *2*, 930–942.
- [5] V. Lyamichev, A. L. Mast, J. G. Hall, J. R. Prudent, M. W. Kaiser, T. Takova, R. W. Kwiatkowski, T. J. Sander, M. de Arruda, D. A. Arco, B. P. Neri, M. A. D. Brow, *Nat. Biotechnol.* **1999**, *17*, 292–296.
- [6] S. Tyagi, F. R. Kramer, *Nat. Biotechnol.* **1996**, *14*, 303–308.
- [7] B. Dubertret, M. Calame, A. J. Libchaber, *Nat. Biotechnol.* **2001**, *19*, 365–370.
- [8] H. Kashida, T. Takatsu, T. Fujii, K. Sekiguchi, X. Liang, K. Niwa, T. Takase, Y. Yoshida, H. Asanuma, *Angew. Chem.* **2009**, *121*, 7178–7181; *Angew. Chem. Int. Ed.* **2009**, *48*, 7044–7047.
- [9] T. Ihara, M. Mukae, *Anal. Sci.* **2007**, *23*, 625–629.
- [10] Y. N. Teo, E. T. Kool, *Chem. Rev.* **2012**, *112*, 4221–4245.
- [11] J. D. Wulfkühle, L. A. Liotta, E. F. Petricoin, *Nat. Rev. Cancer* **2003**, *3*, 267–275.
- [12] Y. Urano, *Anal. Sci.* **2008**, *24*, 51–53.
- [13] J. Li, W. Zhou, X. Ouyang, H. Yu, R. Yang, W. Tan, J. Yuan, *Anal. Chem.* **2011**, *83*, 1356–1362.
- [14] D. C. Harris, B. R. Saks, J. Jayawickramarajah, *J. Am. Chem. Soc.* **2011**, *133*, 7676–7679.
- [15] K. Gorska, A. Manicardi, S. Barluenga, N. Winsinger, *Chem. Commun.* **2011**, *47*, 4364–4366.
- [16] Y. Sato, S. Nishizawa, K. Yoshimoto, T. Seino, T. Ichihashi, K. Morita, N. Teramae, *Nucleic Acids Res.* **2009**, *37*, 1411–1422.
- [17] Y. Sato, T. Ichihashi, S. Nishizawa, N. Teramae, *Angew. Chem.* **2012**, *124*, 6475–6478; *Angew. Chem. Int. Ed.* **2012**, *51*, 6369–6372.
- [18] J. Wu, Y. Zou, C. Li, W. Sicking, I. Piantanida, T. Yi, C. Schmuck, *J. Am. Chem. Soc.* **2012**, *134*, 1958–1961.
- [19] K. Onizuka, Y. Taniguchi, S. Sasaki, *Bioconjugate Chem.* **2009**, *20*, 799–803.
- [20] Y. Taniguchi, R. Kawaguchi, S. Sasaki, *J. Am. Chem. Soc.* **2011**, *133*, 7272–7275.
- [21] N. Tabatadze, C. Tomas, R. McGonigal, B. Lin, A. Schook, A. Routenberg, *Hippocampus* **2012**, *22*, 1228–1241.
- [22] S.-H. Fujishima, R. Yasui, T. Miki, A. Ojida, I. Hamachi, *J. Am. Chem. Soc.* **2012**, *134*, 3961–3964.
- [23] P. Arslan, A. Jyo, T. Ihara, *Org. Biomol. Chem.* **2010**, *8*, 4843–4848.
- [24] M. Mukae, T. Ihara, M. Tabara, A. Jyo, *Org. Biomol. Chem.* **2009**, *7*, 1349–1354.
- [25] T. Ihara, T. Fujii, M. Mukae, Y. Kitamura, A. Jyo, *J. Am. Chem. Soc.* **2004**, *126*, 8880–8881.
- [26] T. Ihara, Y. Kitamura, Y. Tsujimura, A. Jyo, *Anal. Sci.* **2011**, *27*, 585–590.
- [27] Y. Kitamura, T. Ihara, Y. Tsujimura, Y. Osawa, D. Sasahara, M. Yamamoto, K. Okada, M. Tazaki, A. Jyo, *J. Inorg. Biochem.* **2008**, *102*, 1921–1931.
- [28] T. Ihara, T. Wasano, R. Nakatake, P. Arslan, A. Futamura, A. Jyo, *Chem. Commun.* **2011**, *47*, 12388–12390.
- [29] T. Ogoshi, A. Harada, *Sensors* **2008**, *8*, 4961–4982.
- [30] A. Ueno, S. Minato, I. Suzuki, M. Fukushima, M. Ohkubo, T. Osa, F. Hamada, K. Murai, *Chem. Lett.* **1990**, *19*, 605–608.
- [31] R. Corradini, A. Dossena, R. Marchelli, A. Panagia, G. Sartor, M. Saviano, A. Lombardi, V. Pavone, *Chem. Eur. J.* **1996**, *2*, 373–381.

- [32] *Molecular encapsulation: Organic reactions in constrained systems* (Eds.: U. H. Brinker, J.-L. Mieusset), Wiley, Chichester, **2011**.
- [33] A. Kuzuya, T. Ohnishi, T. Wasano, S. Nagaoka, J. Sumaoka, T. Ihara, A. Jyo, M. Komiyama, *Bioconjugate Chem.* **2009**, *20*, 1643–1649.
- [34] H. Takakusa, K. Kikuchi, Y. Urano, T. Higuchi, T. Nagano, *Anal. Chem.* **2001**, *73*, 939–942.
- [35] H.-J. Schneider, A. K. Yatsimirsky, *Principles and Methods in Supramolecular Chemistry*, Wiley, Chichester, **2000**.
- [36] T. Ihara, A. Uemura, A. Futamura, M. Shimizu, N. Baba, S. Nishizawa, N. Teramae, A. Jyo, *J. Am. Chem. Soc.* **2009**, *131*, 1386–1387.
- [37] K. Yoshimoto, S. Nishizawa, M. Minagawa, N. Teramae, *J. Am. Chem. Soc.* **2003**, *125*, 8982–8983.
- [38] B. Rajendar, A. Rajendran, Z. Ye, E. Kanai, Y. Sato, S. Nishizawa, M. Sikorski, N. Teramae, *Org. Biomol. Chem.* **2010**, *8*, 4949–4959.
- [39] Y. Sato, Y. Zhang, T. Seino, T. Sugimoto, S. Nishizawa, N. Teramae, *Org. Biomol. Chem.* **2012**, *10*, 4003–4006.
- [40] B. Rajendar, A. Rajendran, Y. Sato, S. Nishizawa, N. Teramae, *Bioorg. Med. Chem.* **2009**, *17*, 351–359.
- [41] S. Miura, S. Nishizawa, A. Suzuki, Y. Fujimoto, K. Ono, Q. Gao, N. Teramae, *Chem. Eur. J.* **2011**, *17*, 14104–14110.
- [42] A. Rajendran, C. Zhao, B. Rajendar, V. Thiagarajan, Y. Sato, S. Nishizawa, N. Teramae, *Biochim. Biophys. Acta Gen. Subj.* **2010**, *1800*, 599–610.
- [43] C. Zhao, A. Rajendran, Q. Dai, S. Nishizawa, N. Teramae, *Anal. Sci.* **2008**, *24*, 693–695.
- [44] W. A. Baase, W. C. Johnson, Jr., *Nucleic Acids Res.* **1979**, *6*, 797–814.
- [45] C. R. Cantor, P. R. Schimmel, *Biophysical Chemistry: the Behavior of Biological Macromolecules*, W. H. Freeman, New York, **1980**.
- [46] R. E. Dickerson, H. R. Drew, B. N. Conner, R. M. Wing, A. V. Fratini, M. L. Kopka, *Science* **1982**, *216*, 475.
- [47] S. Neidle, *Oxford Handbook of Nucleic Acid Structure*, Oxford University Press, Oxford, **1999**.
- [48] Y. Sato, T. Kageyama, S. Nishizawa, N. Teramae, *Anal. Sci.* **2013**, *29*, 15–19.
- [49] Z. Ye, B. Rajendar, D. Qing, S. Nishizawa, N. Teramae, *Chem. Commun.* **2008**, 6588–6590.
- [50] H. Dodziuk, *Cyclodextrins and Their Complexes*. Wiley-VCH, Weinheim. **2006**.
- [51] F. S. Damos, R. Luz, A. A. Sabino, M. N. Eberlin, R. A. Pilli, L. T. Kubota, *J. Electroanal. Chem.* **2007**, *601*, 181–193.
- [52] K. Fujita, T. Ueda, T. Imoto, I. Tabushi, N. Toh, T. Koga, *Bioorg. Chem.* **1982**, *11*, 108–114.
- [53] C.-X. Wang, Y. Sato, M. Kudo, S. Nishizawa, N. Teramae, *Chem. Eur. J.* **2012**, *18*, 9481–9484.
- [54] T. Russ, W. Ried, F. Ullrich, E. Mutschler, *Arch. Pharm.* **1992**, *325*, 761–767.

Received: March 14, 2013
Published online: ■■■, 0000